$$\Delta C_{f_0}=\overline{C}_{f_0}'-\overline{C}_{f_0}+\frac{W_0}{B_0-T_0}+\frac{2}{\pi}\left\{\log\frac{B_0-T_0}{W_0}+\log\frac{k_0K'}{2\pi}\right\}+O(g). \quad (22)$$

Accordingly, since $\overline{C}_{f_0}'-\overline{C}_{f_0}\to 0$ when $g\to 0$, as we have previously seen, in the limit,

$$\bar{\Delta}C_{f_0}=\frac{K'}{K}+\frac{2}{\pi}\log\frac{kK}{2\pi} \quad (23)$$

where k, K, and K' are defined in (14).

A curve expressing the relationship between $\bar{\Delta}C_{f_0}$ and $W_0/(B_0-T_0)$ is presented in Fig. 3. When $W_0/(B_0-T_0)\to 0$, $K\to\infty$ and $k\to 1$ so that $\bar{\Delta}C_{f_0}$ becomes infinite logarithmically. On the other hand, when $W_0/(B_0-T_0)\to\infty$, $K'\to\infty$ and $k\to 0$ so that $\bar{\Delta}C_{f_0}\to 0$.

For any given value of W_0, B_0, and T_0, $\Delta C_{f_0}<\bar{\Delta}C_{f_0}$ so that values taken from Fig. 3 put an absolute upper limit on the interaction between the symmetrical odd-mode fringing capacitances. Fig. 4 gives two curves of ΔC_{f_0} versus S to illustrate how the general curve can be accurately deduced from information now at hand. The plotted points on the curves between the points marked with circles and triangles were obtained from the expression $\Delta C_{f_0}\approx C_{f_0}'-\overline{C}_{f_0}'+W_0/(B_0-T_0)-T_0/S_0$, which follows from (13) when $\overline{C}_{f_0}'\approx\overline{C}_{f_0}$. This approximation gives the rapidly changing portion of the curves with great accuracy. When the approximate values were compared with the exact values marked with circles (from [2]), where they are least accurate, it was found that for $T=0.4$ the error was of the order of 5×10^{-4} and for $T=0.6$ the error was less than 1×10^{-5}. The values plotted at $S=2$ were obtained from formulas given by Bates [4]. They are actually values for $S=\infty$. It is known however that the presence of the side walls this far from the inner conductor will have a negligible effect on C_{f_0}' and C_{f_0}. Thus the effect on ΔC_{f_0} will be even less.

References

[1] W. J. Getsinger, "Coupled rectangular bars between parallel plates," *IRE Trans. Microwave Theory Tech.*, vol. MTT-10, pp. 65–72, Jan. 1962.
[2] H. J. Riblet, "The exact dimensions of a family of rectangular coaxial lines with given impedance," *IEEE Trans. Microwave Theory Tech.*, vol. MTT-20, pp. 538–541, Aug. 1972.
[3] F. Bowman, *Introduction to Elliptic Functions with Applications*. New York: Dover, 1961, pp. 83–84.
[4] R. H. T. Bates, "The characteristic impedance of the shielded slab line," *IRE Trans. Microwave Theory Tech.*, vol. MTT-4, pp. 28–33, Jan. 1956.

Swept Frequency Impedance Indicator Using Directional Couplers

SHUNICHIRO EGAMI

***Abstract*—A swept frequency impedance indicator which consists of directional couplers and detectors is described. Experimental equipment was made at a 17.5–19.5-GHz band, and successfully operated.**

Introduction

Swept frequency impedance measurement is very useful in the design and analysis of microwave devices. The method described here is intended for swept frequency impedance measurement in the millimeter waveband.

Several impedance-indicating methods applicable to the millimeter waveband are frequency dependent inherently [1], [2], or magic T with relatively narrow bandwidth were used [3]. The method described here has no frequency dependence on its operation and the swept frequency band is limited by the bandwidth of directional couplers, detectors, and circulators, if used. Frequency of measurement can be raised easily to the millimeter waveband because couplers and detectors can operate equally at this band.

Circuit for the Measurement

The coupled output of a directional coupler has a 90° phase difference with the uncoupled output. This phase shift depends on the directivity of the coupler and is independent of the frequency. This property is applied in this method. Fig. 1 shows the configuration for swept frequency measurement. $C3$ is the power divider which splits the input power with negligible frequency response. $C4$ is the coupler which makes the 90° phase difference to get voltages proportional to $r\cos\phi$ and $r\sin\phi$ (r, ϕ: amplitude and phase of the reflection coefficient of the device under test). In this configuration the length of line $C3$–$C6$ and $C3$-$L2$-$C5$ must be the same. This is adjusted by the phase shifter or line strecher $L2$. (This adjustment can be correctly carried out by connecting a short-ended long line as a device under test, and making the locus on the CRT circle.)

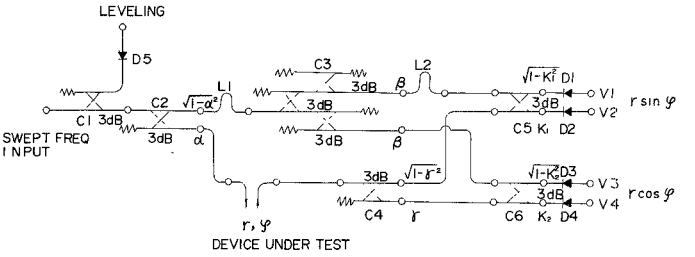

Fig. 1. Circuit for swept frequency measurement.

Then, changing the length of line $L1$, the measurement reference plane can be changed as desired. If the magnitude of the coupling of the couplers is designated as in Fig. 1, differences in the output voltage are given as follows.

$$V_1-V_2=(k_1^2-\tfrac{1}{2})\{r^2(1-\alpha^2)\beta^2-\alpha^2(1-\gamma^2)\}+2\alpha\sqrt{1-\alpha^2}\cdot k_1\sqrt{1-k_1^2}\cdot\sqrt{1-\gamma^2}\cdot\beta\cdot r\cos\phi \quad (1)$$

$$V_3-V_4=(k_2^2-\tfrac{1}{2})\{r^2(1-\alpha^2)\beta^2-\alpha^2\gamma^2\}+2\alpha\sqrt{1-\alpha^2}\cdot k_2\sqrt{1-k_2^2}\cdot\gamma\cdot\beta\cdot r\sin\phi. \quad (2)$$

If $k_1=k_2=1/\sqrt{2}$ and α, β, γ are constant over the swept frequency band, voltage proportional to $r\cos\phi$ and $r\sin\phi$ can be obtained.

Error Consideration

Amplitude of the reflection coefficient on the CRT may be affected by:

1) nonuniform power level of the swept frequency input;
2) nonuniform frequency response of the detector;
3) nonuniform frequency response of the coupler.

The effect of 1) and 2) can be nullified by "leveling" of the sweep oscillator output using a 3-dB coupler ($C1$) and detectors ($D1\sim D5$) with matched characteristics.

Since the 3-dB coupler has reverse frequency response at the coupled and uncoupled output, the effect of 3) on $C2$, $C5$, and $C6$ can be neglected, as understood by (1) and (2). Frequency response of $C3$ can also be nullified using the configuration of Fig. 1. Eventually, the effect of 3) can be restricted to $C4$. So, care must be taken to get a flat frequency response at $C4$. (Change of radius is 1.2 percent/0.1 dB.) Position of the locus on the CRT is determined by the first terms of (1) and (2). Deviation of k_1 and k_2 from $1/\sqrt{2}$ makes the small shift of the locus by the frequency. So, care must be taken to make k_1 and k_2 equal to $1/\sqrt{2}$. In this method, correctness of the phase measurement is determined by the phase error of the couplers.

This can be very small if the directivity of the couplers is sufficiently high, and mismatch of the circuit is made small. Phase error of the coupler at the matched condition is given by the following equation.

$$|\delta\phi|<\frac{1}{2}\cdot\frac{1}{1-k^2}\cdot\frac{1}{D}$$

where

$\delta\phi$ phase error from $\pi/2$ (radian);
k magnitude of coupling;
D directivity of the coupler.

If $D=35$ dB, $\delta\phi$ does not exceed 0.015°. But this may be degraded by mismatch of the circuit. Since the VSWR of the millimeter-waveband detectors is high, it is necessary to lower this about 1.2 to get phase error smaller than 1° [4].

Result of Experiment

The configuration shown in Fig. 1 was constructed for the 18-GHz band. Directivity of the coupler was over 35 dB in the 15–21-GHz band. A circulator, one port of which was connected by a movable short, was used as the line stretcher $L1$. $L2$ was a simple phase shifter fixed at a suitable point. Reflection from the device under test can be derived by a circulator or a coupler. In this case, a circu-

Manuscript received December 11, 1972; revised June 6, 1973.
The author is with the Electrical Communication Laboratory, Nippon Telegraph and Telephone Public Corp., 1-2354 Take Yokisuka-shi 238-03, Japan.

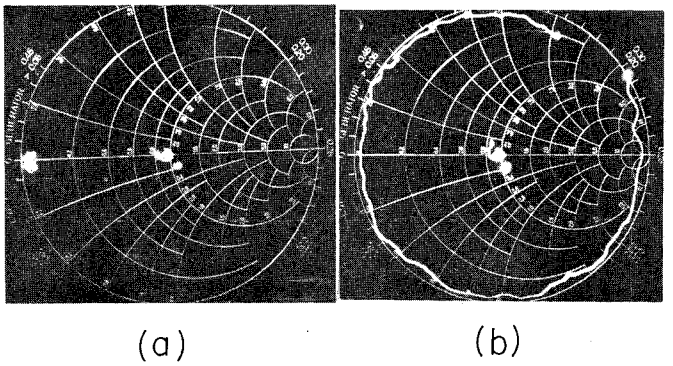

Fig. 2. (a) Impedance locus of the short-ended guide when the reference plane is situated at the shorted point. The impedance locus is concentrated to the $0+j0$-Ω point. The locus is at the center when a matched load is connected. (b) Impedance locus of a short-ended waveguide several centimeters long. The swept frequency is 17.5–19.5 GHz.

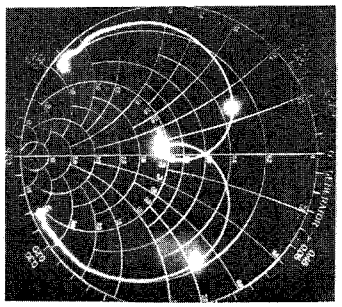

Fig. 3. Impedance locus of the 3-stage Chebyshev waveguide bandpass filter. The swept frequency is 18.0–19.0 GHz. The marker indicates 18.0 ± 0.1 GHz. The reference plane is situated at the first iris of the filter.

lator was used. Due to the frequency limit of the circulator, sweep frequency range is limited to 17.5–19.5 GHz. Fig. 2(a) shows the impedance locus of the short-ended guide when the reference plane is situated at this shorted point. The locus is concentrated to the $0+j0$-Ω point, which shows the correctness of this method. The locus was on the center of the CRT when a matched load was connected as the device under test.

Fig. 2(b) shows the impedance locus of a short-ended waveguide several centimeters long. Fig. 3 shows the impedance locus of the 3-stage Chebyshev waveguide bandpass filter. In this case, the reference plane was located at the first iris of the filter. Simplicity and ease of manufacture in the millimeter waveband are the features of this method.

References

[1] A. L. Samuel, "An oscillographic method of presenting impedances on the reflection-coefficient plane," *Proc. IRE*, vol. 35, pp. 1279–1283, Nov. 1947.
[2] S. B. Cohn, "Impedance measurement by means of a broadband circular-polarization coupler," *Proc. IRE*, vol. 42, pp. 1554–1558, Oct. 1954.
[3] P. I. Somlo, "The locating reflectometer," *IEEE Trans. Microwave Theory Tech.*, vol. MTT-20, pp. 105–112, Feb. 1972.
[4] G. E. Schafer, "Mismatch errors in microwave phase shift measurements," *IEEE Trans. Microwave Theory Tech.*, vol. MTT-8, pp. 617–622, Nov. 1960.

High-Power Frequency Multiplier Using MIS Varactors

F. SCHUMACHER

***Abstract*—The experiment described demonstrates the applicability of MIS varactors in microwave power circuits. A frequency doubler with 55-percent overall efficiency and pulsed output power of 5.5 W at 5.4 GHz with a duty cycle of 50 percent has been built by using two MIS varactors in parallel. The multiplier has a coaxial low-pass filter at the input and a waveguide output, allowing a 3-dB bandwidth of 8 percent.**

Manuscript received February 12, 1973; revised May 21, 1973.
The author is with the Institut für Hochfrequenztechnik, Technische Universität Braunschweig, D-33 Braunschweig Postfach 3329, Germany.

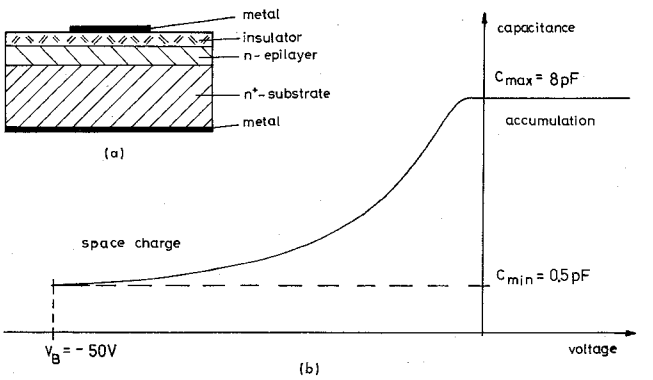

Fig. 1. An MIS varactor. (a) Structure. (b) *CV* characteristic.

TABLE I
MIS Varactor Specifications

Substrate thickness	120 μm
Substrate resistivity	0.011 Ωcm
Epitaxial layer thickness	4 μm
Epitaxial resistivity	0.8 Ωcm
Insulator	100 Å SiO_2 + 800 Å Si_3N_4
Contact diameter	150 μm
Max. capacitance	8 pF
Min. capacitance	0.5 pF
Series resistance	3.2 Ω
Cutoff frequency	94 GHz
Breakdown voltage	50 V
Insulator breakdown voltage	60 V

The application of MIS varactors in frequency multipliers was first described in [1]. Experiments with an upconverter using MIS varactors [2] showed the MIS varactor to be, in many respects, superior to the charge-storage varactor. This short paper describes the application of a MIS varactor in a frequency multiplier at high power levels.

The structure of the MIS varactor is shown in Fig. 1(a). An epitaxial silicon wafer with a highly doped substrate and a thin epitaxial layer is used. Upon this an insulating layer of silicon dioxide and silicon nitride is deposited; a titanium–gold contact is then evaporated by using photoresist techniques.

Fig. 1(b) shows the high-frequency large-signal capacitance–voltage (*CV*) characteristic of the MIS varactors used. With the exception of a finite accumulation capacitance, the *CV* characteristic is similar to that of a charge-storage varactor with constant doping level. The main advantage is that the MIS varactor in this application is a pure majority-carrier device [3]–[5]. No minority-carrier transit time or recombination effects, which would reduce the efficiency and limit the drive level, are present. The MIS varactor therefore allows good efficiencies at higher drive levels, resulting in higher power capability.

The specifications of the MIS varactors are listed in Table I. Since the theoretical resistance of the epitaxial layer is 1.6 Ω, the devices have relatively high parasitic losses. One reason may be the high substrate thickness of 120 μm, which also results in a high thermal resistance. Further progress in technology, e.g., the upside-down technique, and special optimization of varactor parameters for power applications are expected to lead to significantly better devices. A cutoff frequency of 160 GHz and a breakdown voltage of 70 V should be attainable.

Two of these devices have been mounted in parallel in the frequency doubler shown in Fig. 2. This doubler was developed as a simple low-frequency model for further scaling up to the *Ku*-band. 2.7-GHz power is introduced to the varactor diodes from the coaxial input. A transforming low-pass filter within this line bars 5.4-GHz